

**Science**

 AAAS

**Mechanism of Two Classes of Cancer Mutations in the Phosphoinositide 3-Kinase Catalytic Subunit**

Nabil Miled, *et al.*

*Science* **317**, 239 (2007);

DOI: 10.1126/science.1135394

***The following resources related to this article are available online at [www.sciencemag.org](http://www.sciencemag.org) (this information is current as of December 8, 2007):***

**Updated information and services**, including high-resolution figures, can be found in the online version of this article at:

<http://www.sciencemag.org/cgi/content/full/317/5835/239>

**Supporting Online Material** can be found at:

<http://www.sciencemag.org/cgi/content/full/317/5835/239/DC1>

A list of selected additional articles on the Science Web sites **related to this article** can be found at:

<http://www.sciencemag.org/cgi/content/full/317/5835/239#related-content>

This article **cites 29 articles**, 17 of which can be accessed for free:

<http://www.sciencemag.org/cgi/content/full/317/5835/239#otherarticles>

This article appears in the following **subject collections**:

Biochemistry

<http://www.sciencemag.org/cgi/collection/biochem>

Information about obtaining **reprints** of this article or about obtaining **permission to reproduce this article** in whole or in part can be found at:

<http://www.sciencemag.org/about/permissions.dtl>

30. We thank M. Kwan, S. Sang, B. Doidge, D. Muir, J. Arnot, J. Armitage, M. Fischer, N. Crewe, and M. Gibbs.

We acknowledge the Natural Sciences and Engineering Research Council of Canada and Environment Canada's Northern Ecosystems Initiative for financial support, Fisheries and Oceans Canada for chemical analysis support, and

northern Quebec Inuit communities of Umiujaq and Inukjuaq for assistance with collection of field samples.

#### Supporting Online Material

www.sciencemag.org/cgi/content/full/317/5835/236/DC1  
Materials and Methods

Figs. S1 to S6  
Tables S1 to S11  
References

1 December 2006; accepted 8 June 2007  
10.1126/science.1138275

# Mechanism of Two Classes of Cancer Mutations in the Phosphoinositide 3-Kinase Catalytic Subunit

Nabil Miled,<sup>1\*†</sup> Ying Yan,<sup>2\*</sup> Wai-Ching Hon,<sup>1</sup> Olga Perisic,<sup>1</sup> Marketa Zvelebil,<sup>3</sup> Yuval Inbar,<sup>4</sup> Dina Schneidman-Duhovny,<sup>4</sup> Haim J. Wolfson,<sup>4</sup> Jonathan M. Backer,<sup>2‡</sup> Roger L. Williams<sup>1‡</sup>

Many human cancers involve up-regulation of the phosphoinositide 3-kinase PI3K $\alpha$ , with oncogenic mutations identified in both the p110 $\alpha$  catalytic and the p85 $\alpha$  regulatory subunits. We used crystallographic and biochemical approaches to gain insight into activating mutations in two noncatalytic p110 $\alpha$  domains—the adaptor-binding and the helical domains. A structure of the adaptor-binding domain of p110 $\alpha$  in a complex with the p85 $\alpha$  inter-Src homology 2 (inter-SH2) domain shows that oncogenic mutations in the adaptor-binding domain are not at the inter-SH2 interface but in a polar surface patch that is a plausible docking site for other domains in the holo p110/p85 complex. We also examined helical domain mutations and found that the Glu<sup>545</sup> to Lys<sup>545</sup> (E545K) oncogenic mutant disrupts an inhibitory charge-charge interaction with the p85 N-terminal SH2 domain. These studies extend our understanding of the architecture of PI3Ks and provide insight into how two classes of mutations that cause a gain in function can lead to cancer.

Phosphoinositide 3-kinases and their lipid product, phosphatidylinositol-(3,4,5)-trisphosphate [PtdIns(3,4,5)P<sub>3</sub>], play key roles in a variety of cellular processes (1–3). Aberrations in PtdIns(3,4,5)P<sub>3</sub> levels, either through activation of PI3Ks or through inactivation of lipid phosphatase PTEN, occur frequently in numerous forms of cancers. For example, recent data suggest that at least 50% of human breast cancers involve mutations in either PI3K $\alpha$  or PTEN (4, 5). Broad-spectrum PI3K inhibitors such as LY294002 or wortmannin result in increased apoptosis, decreased proliferation, and reduced metastasis in vitro and in tumor models [reviewed in (6–8)]. Understanding the structural mechanisms of PI3K regulation may facilitate development of isozyme-specific therapeutics.

The class IA PI3Ks are obligate heterodimers (9), consisting of a p110 catalytic subunit and a regulatory subunit. Any of the three class IA catalytic subunits (p110 $\alpha$ , p110 $\beta$ , and p110 $\delta$ )

can bind any of the p85-related regulatory subunits. Regulatory subunits have multiple roles in the function of PI3K: down-regulation of the basal activity, stabilization of the catalytic subunit, activation downstream of receptor tyrosine kinases, and sequential activation by tyrosine kinases and Ras (10–13). Common to all regulatory subunits are two SH2 domains (nSH2 and cSH2) that flank an intervening domain (iSH2), and common to all catalytic subunits are the N-terminal adaptor-binding domain (ABD), the Ras-binding domain (RBD), the putative membrane-binding domain (C2), and the helical and catalytic domains (Fig. 1A). The iSH2 domain is responsible for tight binding to the ABD (14). The nSH2 and cSH2 domains bind phosphorylated tyrosines in Tyr-X-X-Met motifs found in activated receptors and adaptor proteins, and this interaction activates the heterodimeric PI3K. The nSH2-iSH2 unit constitutes the minimal fragment capable of regulating the PI3K activity (15): It both inhibits the basal activity and facilitates activation by binding phosphotyrosine peptides. In contrast, the isolated iSH2 only minimally affects the PI3K activity, although it tightly binds the p110 subunit.

A number of studies have identified a high frequency of somatic point mutations in the gene encoding the p110 $\alpha$  catalytic subunit in different human cancers (16, 17). An increased lipid kinase activity in vitro and the ability to induce oncogenic transformation in vivo were shown both for the most frequently mutated, “hotspot” residues (16, 18–20) and for 14 rare cancer-specific mutations in p110 $\alpha$  (21). The

cancer-specific mutations can be grouped into four classes defined by the four domains of the catalytic subunit in which they occur—the ABD, C2, helical, and catalytic domains—and it has been proposed that these classes may increase PI3K activity by different mechanisms (21, 22). Hotspot mutations in the catalytic domain cluster around the “activation loop” involved in substrate recognition (23) and are likely to share a common mechanism (21). The ABD binds tightly to the regulatory subunit, the C2 domain is thought to interact with the plasma membrane, and the helical domain appears to act as a rigid scaffold around which the RBD, C2, and catalytic domains are mounted (24). The catalytic and C2 domain mutations may up-regulate PI3K by increasing the affinity for substrate-containing membranes. However, it is not immediately clear what might be the mechanism of helical domain mutations. We used structural and biochemical approaches to understand the basis for gain-of-function mutations in the ABD and helical domains of p110 $\alpha$ . Because the ABD is the only p110 domain for which there is no known structure, we crystallized it in a complex with the iSH2 domain from p85. This structure suggested a rough preliminary model for the p110/p85 heterodimer, which led us to hypothesize that the nSH2 domain might contact the helical domain. To understand how helical domain oncogenic mutations function, we created a series of site-specific mutations in the nSH2 domain, resulting in an adaptor subunit that specifically counteracts the p110 helical domain hotspot E545K mutant.

We determined the crystal structure of a complex between the bovine p110 $\alpha$  ABD (residues 1 to 108) and the human p85 $\alpha$  iSH2 domain (residues 431 to 600) at 2.4 Å resolution (25), revealing the interaction of the small, globular ABD (35 by 25 by 15 Å) with one end of the long, rodlike iSH2 (115 Å long) (Fig. 1B). The ABD is similar to many ubiquitin-like domains: It superimposes on ubiquitin with a root mean square deviation of 1.4 Å for 60 out of 76 residues (Fig. 1C). The  $\beta$ -grasp fold of both the ABD and ubiquitin is a common fold, and neither sequence nor function suggests a common origin for the ABD and ubiquitin. The ABD ranks as one of the least conserved domains among class I catalytic subunits. Conversely, the iSH2 domain is highly conserved in vertebrates, sharing >90% sequence similarity from human to zebrafish (fig. S1). Despite a lack of sequence similarity, secondary and tertiary structure predictions for the class IB p110 $\gamma$  ABD are consistent with a ubiquitin-like fold, similar to the class IA p110 ABD. However, the greater sequence divergence of the p110 $\gamma$  ABD makes it

<sup>1</sup>Medical Research Council Laboratory of Molecular Biology, Hills Road, Cambridge CB2 2QH, UK. <sup>2</sup>Department of Molecular Pharmacology, Albert Einstein College of Medicine, Bronx, NY 10461, USA. <sup>3</sup>Ludwig Institute for Cancer Research, University College London, London W1W 7BS, UK. <sup>4</sup>School of Computer Science, The Raymond and Beverly Sackler Faculty of Exact Sciences, Tel Aviv University, Tel Aviv 69978, Israel.

\*These authors contributed equally to this work.

†Present address: Laboratoire de Biochimie et de Génie Enzymatique des Lipases, Ecole Nationale d'Ingenieurs Sfax, Route Soukra BPW, 3038 Sfax, Tunisia.

‡To whom correspondence should be addressed. E-mail: rlw@mrc-lmb.cam.ac.uk (R.L.W.); backer@aecom.yu.edu (J.M.B.)

unable to bind the iSH2 domain. Consistent with previous studies (26), the p85 $\alpha$  iSH2 domain consists of two helices,  $\alpha$ 1 and  $\alpha$ 2, that form a long, antiparallel coiled coil followed by the short  $\alpha$ 3 helix (Fig. 1B).

The ABD/iSH2 interface is large, burying 2284 Å<sup>2</sup> surface area, with the concave face of the ABD  $\beta$  sheet interacting with the coiled-coil helices of the iSH2 (Fig. 1, B and E). Most of the interactions with the ABD are formed by the iSH2 helix  $\alpha$ 1, which contacts the ABD with seven of its turns, whereas only three turns of iSH2 helix  $\alpha$ 2 interact with the ABD. Central to the ABD/iSH2 interface is the surface encompassing the strands  $\beta$ 1 to  $\beta$ 2 of the ABD, which contains the conserved 25-Leu-Leu-Pro-X-Gly- $\phi$ -31 motif, where  $\phi$  denotes a hydrophobic residue (Fig. 1, D and E). This motif forms a loop that through both its side chains and backbone contacts two conserved iSH2 residues, Gln<sup>497</sup> and Asn<sup>527</sup>, one on each long helix of the domain. Among all residues at the interface, the side chains of these two polar iSH2 residues engage in the greatest number of intersubunit contacts. Overall, about three-quarters of the ABD/iSH2 interactions are van der Waals contacts, and most of them involve exposed hydrophobic side chains (fig. S1). At the periphery of the interface are two salt links, Glu<sup>23</sup><sub>ABD</sub>/Arg<sup>534</sup><sub>iSH2</sub> and Arg<sup>79</sup><sub>ABD</sub>/Glu<sup>496</sup><sub>iSH2</sub>; however, site-specific mutagenesis of the individual charged residues to Ala did not eliminate binding in vitro. This is consistent with the very high affinity of the iSH2 domain for the ABD (14, 27). Other iSH2-contacting sites include the  $\alpha$ 1/ $\beta$ 3, the  $\beta$ 3/ $\beta$ 4, and the  $\beta$ 4/ $\beta$ 5 loops of ABD.

Among rare cancer-specific mutations in p110, there are three residues that map to the ABD—Arg<sup>38</sup>, Arg<sup>88</sup>, and Pro<sup>104</sup>. Recently, it was shown the R38H (28) mutation induces oncogenic transformation of avian cells, although with weak efficiency (21). None of these residues are at the interface between the ABD and the iSH2 domain. Analysis with ConSurf (29) shows that there is a highly conserved ABD surface patch outside the conserved ABD/iSH2 interface (Fig. 2A). This patch, formed by the  $\beta$ 4/h3 region and the  $\beta$ 2/ $\alpha$ 1 loop in the ABD (Fig. 2 and fig. S1), consists predominately of polar residues, including two of the three ABD residues whose mutation is linked with cancer, Arg<sup>38</sup> and Arg<sup>88</sup>. It represents a plausible docking site for other domains in the rest of the p110/p85 complex. Mutations in this surface may affect the relationship of the ABD with respect to the catalytic core. This could reorient the adaptor subunit with respect to the p110 subunit or change the orientation of the enzyme on the membrane.

A minimal regulatory p85 fragment consisting of nSH2 and iSH2 (p85ni) readily inhibits activity of the wild-type p110 $\alpha$  (Fig. 3A), suggesting an undefined inhibitory p85-p110 contact (30). Hypothesizing that the helical domain might be a good candidate for the inhibitory nSH2 binding, we looked at the effect of onco-

genic mutants in the helical domain. We found that the p85ni regulatory fragment does not inhibit p110 $\alpha$  helical domain oncogenic mutants

E542K, E545K, or Q546K in vitro (Fig. 3A). Because all of these helical domain mutations increase the positive charge on the surface of the

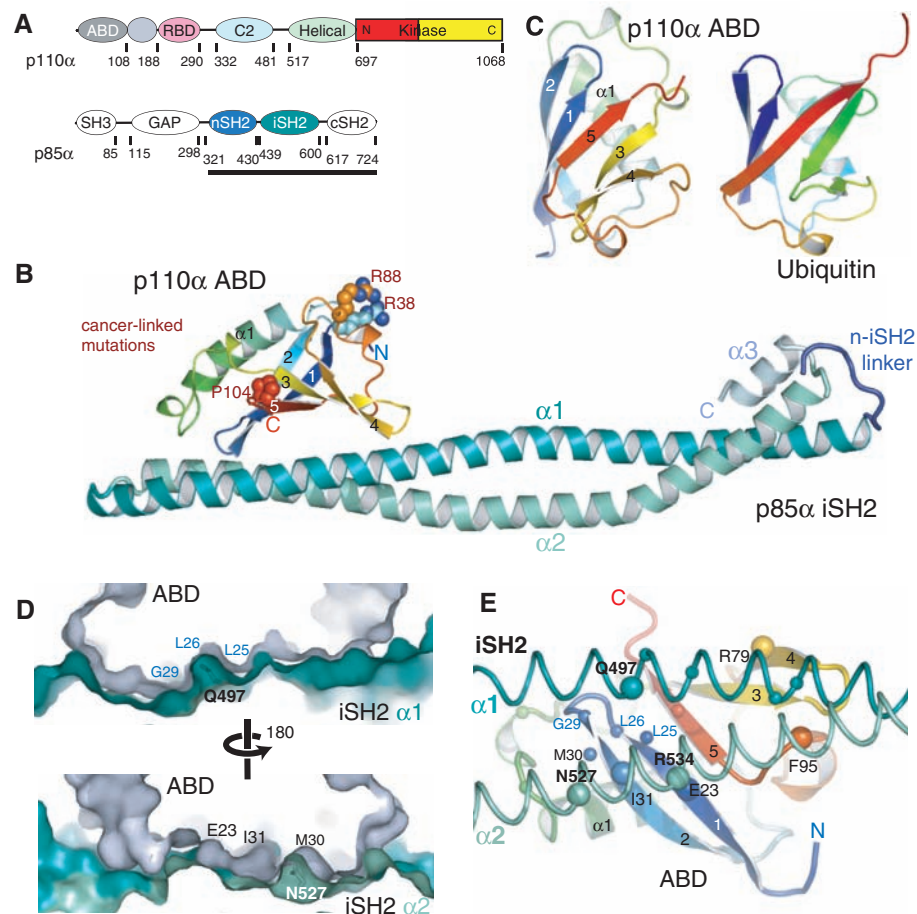


**Fig. 1.** Structure of a class IA PI3K heterodimerization core. (A) Domain organization of PI3K catalytic (classes IA and IB) and regulatory (class IA only) subunits. N and C, N- and C-terminal lobes of the kinase domain, respectively; GAP, Rho-GAP domain. (B) Ribbon representation of ABD/iSH2 heterodimer. The three ABD residues identified as somatic mutations in colon cancers (shown in spheres) are not in the ABD/iSH2 interface. (C) The ABD has a ubiquitin-like fold. (D) A cross-section through the ABD/iSH2 interface showing the surface complementarity. (E) Underside view of the heterodimer interface showing residues that contribute substantially to the binding.  $\alpha$  atoms of residues forming prominent interactions with the iSH2 (contributing more than nine interatomic contacts, interatomic distance < 3.8 Å) are shown as large spheres. Smaller spheres represent residues involved in less extensive interactions (four to six interatomic contacts).

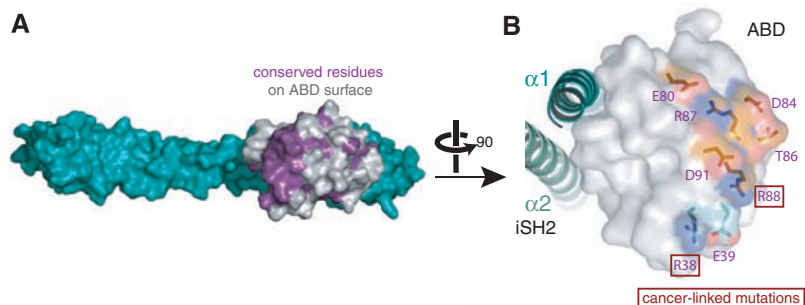


**Fig. 2.** A model of the minimal p110/p85 complex, showing the locations of rare cancer-specific mutations in the ABD. (A) Two ABD residues that are mutated in colon cancers map to a conserved, non-iSH2-binding surface patch (purple). (B) A view of the ABD/iSH2 complex rotated 90° around a vertical axis, showing conserved residues on the ABD surface and cancer-specific mutation sites (boxed).

helical domain, we speculated that there might be an inhibitory interaction between the nSH2 and the wild-type helical domain involving a charge-charge interaction between an acidic patch on the helical domain and a basic residue on the surface of the nSH2 domain. We singly mutated each of the lysine or arginine residues on the surface of the nSH2 domain into glutamate.

Among these mutants, only the p85ni-R340E and p85ni-K379E mutants did not inhibit the wild-type p110 $\alpha$  (Fig. 3B). The loss of inhibition for R340E and K379E suggests that these residues are involved in an inhibitory contact with the catalytic subunit. Consistent with this, the p85ni-K379E mutant inhibits the p110 $\alpha$ -E545K oncogenic mutant, whereas the wild-

type p85ni does not, suggesting that the charge reversal has reestablished the critical inhibitory interaction (Fig. 3C).

The p85 residues Arg<sup>340</sup> and Lys<sup>379</sup> are part of the phosphopeptide-binding surface on the nSH2 domain. Both are in direct contact with bound phosphopeptide in crystal structures of two nSH2/phosphotyrosine-peptide complexes (31), suggesting that the phosphopeptide activates the enzyme by competing with the inhibitory contact. A tandem Tyr-X-X-Met phosphopeptide from the Tyr<sup>608</sup>/Tyr<sup>628</sup> region of insulin receptor substrate 1 (IRS-1) roughly doubled the activation of the wild-type p110 $\alpha$ /p85ni heterodimer but did not activate the p110 $\alpha$ -E545K/p85ni complex (Fig. 3D). Figure 4 suggests how binding of the nSH2 domain to the p110 $\alpha$  helical domain and to the phosphopeptide would be mutually exclusive. Currently, it is not clear how the nSH2 inhibits the wild-type enzyme. The helical domain interacts with the catalytic domain across a broad surface. The contact of the nSH2 domain with the helical domain might trigger a conformational change in the catalytic domain to affect the activity allosterically, or it may influence the orientation of the catalytic domain on the substrate-containing membrane.

The ABD/iSH2 crystal structure completes the architectural account of the whole p110 catalytic subunit and shows that oncogenic mutations in the ABD are not in the interface with the p85 regulatory subunit. Our results also suggest an unexpected function for the helical domain. A rationally designed nSH2 mutant counteracts the gain-of-function oncogenic p110 $\alpha$ -E545K mutation, supporting the proposal that the p85 inhibition of p110 $\alpha$  occurs through a charge-charge interaction between the helical domain and the p85ni. The crystallographic structures combined with the mutational analyses have enabled us to propose a rough partial model for the p110/p85 complex (25), but ongoing studies by nuclear magnetic resonance, electron paramagnetic resonance, and crystallography will be required to refine any such model.

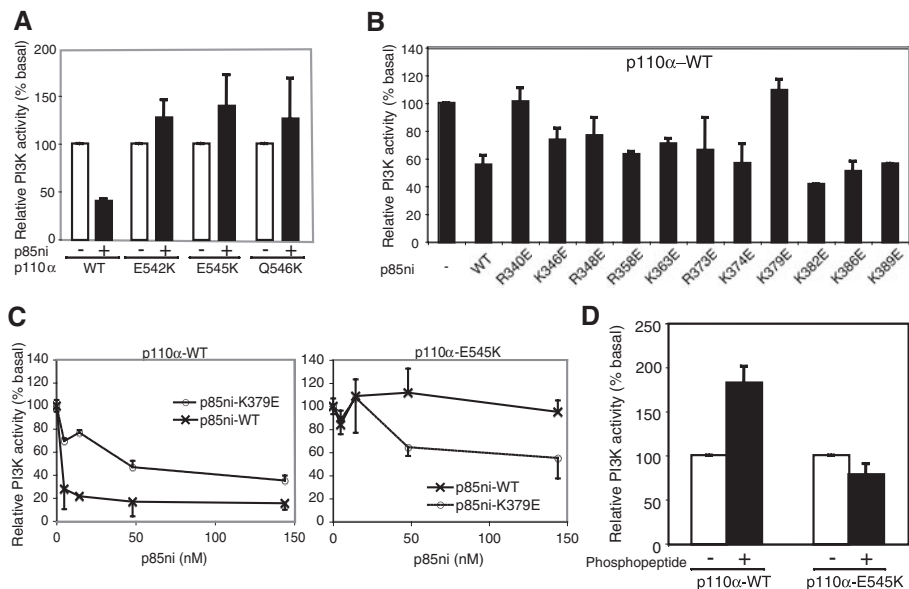
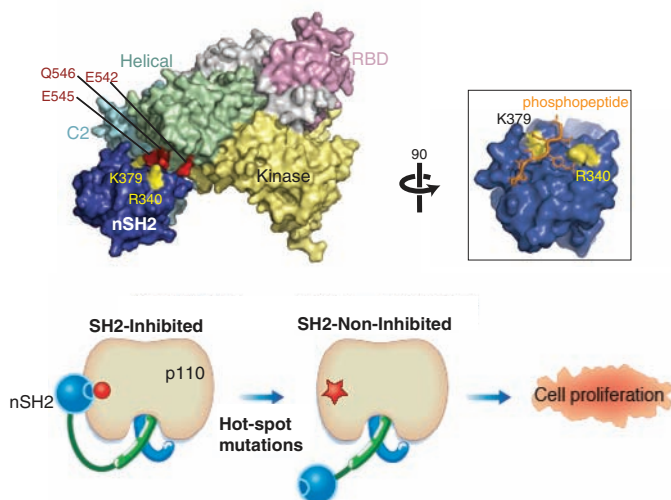


**Fig. 3.** Helical domain oncogenic mutants of p110 $\alpha$  eliminate an autoinhibitory contact with the p85 nSH2 domain. **(A)** PI3K activity of the three p110 $\alpha$  helical domain mutants was not inhibited by the p85ni fragment. Equal amounts of protein were assayed and the catalytic subunits had similar specific activities (fig. S3) (25). WT, wild type. **(B)** Charge-reversal mutagenesis screening of basic surface residues in the nSH2. **(C)** Simultaneous charge-reversal in p110 $\alpha$  and p85ni restored inhibition, suggesting direct interaction between the p110 $\alpha$  helical domain and the p85 $\alpha$  nSH2 domain. A titration series was carried out for both the wild-type (left) and E545K mutant (right) p110 subunits to ascertain that the inhibition was at saturating levels of p85ni. **(D)** Binding of IRS-1 phosphotyrosine peptide activates wild-type p110 $\alpha$ /p85ni but not p110-E545K/p85ni (25). [(A) to (D)] Lipid kinase assays were performed with Myc-p110 $\alpha$  produced in transfected human embryonic kidney 293 cells (A) or baculovirus-infected Sf9 cells [(B) to (D)], incubated with or without excess p85ni [expressed in *Escherichia coli* (25)]. Basal activity refers to p110 $\alpha$  activity in the absence of p85ni. Results are means from three to four experiments [(A) and (B)] or are representative of two experiments, each carried out in triplicate [(C) and (D)].

**Fig. 4.** A model showing the inhibitory contact between the nSH2 domain and the helical domain of p110 $\alpha$  near the site of the helical domain hotspot mutations. [The p110 $\alpha$  catalytic core was modeled on the p110 $\gamma$  catalytic core (24).] Arg<sup>340</sup> and Lys<sup>379</sup> are part of a highly conserved phosphopeptide-binding surface on nSH2. Binding of nSH2 to the p110 $\alpha$  helical domain and to phosphopeptide are mutually exclusive (boxed image).



**References and Notes**

1. L. C. Cantley, *Science* **296**, 1655 (2002).
2. B. Vanhaesebroeck et al., *Annu. Rev. Biochem.* **70**, 535 (2001).
3. M. P. Wymann, M. Zvelebil, M. Laffargue, *Trends Pharmacol. Sci.* **24**, 366 (2003).
4. J. Luo, B. D. Manning, L. C. Cantley, *Cancer Cell* **4**, 257 (2003).
5. L. H. Saal et al., *Cancer Res.* **65**, 2554 (2005).
6. R. Wetzker, C. Rommel, *Curr. Pharm. Des.* **10**, 1915 (2004).
7. M. P. Wymann, R. Marone, *Curr. Opin. Cell Biol.* **17**, 141 (2005).
8. P. Workman, *Biochem. Soc. Trans.* **32**, 393 (2004).
9. B. Geering, P. R. Cutillas, G. Nock, S. I. Gharbi, B. Vanhaesebroeck, *Proc. Natl. Acad. Sci. U.S.A.* **104**, 7809 (2007).
10. J. Yu et al., *Mol. Cell. Biol.* **18**, 1379 (1998).
11. K. Okkenhaug, B. Vanhaesebroeck, *Sci. STKE* **2001**, pe1 (2001).
12. C. Jimenez, C. Hernandez, B. Pimentel, A. C. Carrera, *J. Biol. Chem.* **277**, 41556 (2002).

13. C. L. Carpenter *et al.*, *J. Biol. Chem.* **268**, 9478 (1993).
14. R. Dhand *et al.*, *EMBO J.* **13**, 511 (1994).
15. J. Yu, C. Wjasow, J. M. Backer, *J. Biol. Chem.* **273**, 30199 (1998).
16. Y. Samuels *et al.*, *Science* **304**, 554 (2004).
17. A. G. Bader, S. Kang, L. Zhao, P. K. Vogt, *Nat. Rev. Cancer* **5**, 921 (2005).
18. S. Kang, A. G. Bader, P. K. Vogt, *Proc. Natl. Acad. Sci. U.S.A.* **102**, 802 (2005).
19. T. Ikenoue *et al.*, *Cancer Res.* **65**, 4562 (2005).
20. S. J. Isakoff *et al.*, *Cancer Res.* **65**, 10992 (2005).
21. M. Gymnopoulos, M. A. Elstiger, P. K. Vogt, *Proc. Natl. Acad. Sci. U.S.A.* **104**, 5569 (2007).
22. L. Stephens, R. Williams, P. Hawkins, *Curr. Opin. Pharmacol.* **5**, 357 (2005).
23. L. Pirola *et al.*, *J. Biol. Chem.* **276**, 21544 (2001).
24. E. H. Walker, O. Perisic, C. Ried, L. Stephens, R. L. Williams, *Nature* **402**, 313 (1999).
25. Materials and methods are available as supporting material on *Science* Online.
26. Z. Fu, E. Aronoff-Spencer, J. M. Backer, G. J. Gerfen, *Proc. Natl. Acad. Sci. U.S.A.* **100**, 3275 (2003).
27. W. Elis, E. Lessmann, M. Oelgeschlager, M. Huber, *Biol. Chem.* **387**, 1567 (2006).
28. Single-letter abbreviations for the amino acid residues are as follows: A, Ala; C, Cys; D, Asp; E, Glu; F, Phe; G, Gly; H, His; I, Ile; K, Lys; L, Leu; M, Met; N, Asn; P, Pro; Q, Gln; R, Arg; S, Ser; T, Thr; V, Val; W, Trp; and Y, Tyr.
29. M. Landau *et al.*, *Nucleic Acids Res.* **33**, W299 (2005).
30. S. C. Shekar *et al.*, *J. Biol. Chem.* **280**, 27850 (2005).
31. R. T. Nolte, M. J. Eck, J. Schlessinger, S. E. Shoelson, S. C. Harrison, *Nat. Struct. Biol.* **3**, 364 (1996).
32. We thank M. Waterfield and B. Vanhaesebroeck for the p110 $\alpha$  plasmid, A. McCarthy for help at European Synchrotron Radiation Facility beamline ID14-4, and M. Girvin and G. Gerfen for helpful discussions. The work was supported by AstraZeneca (R.L.W.), Medical Research Council (R.L.W.), and NIH GM55692 (J.M.B.).

#### Supporting Online Material

www.sciencemag.org/cgi/content/full/317/5835/239/DC1

Materials and Methods

Figs. S1 to S5

Table S1

References

21 September 2006; accepted 31 May 2007

10.1126/science.1135394

# Postreplicative Formation of Cohesion Is Required for Repair and Induced by a Single DNA Break

Lena Ström,<sup>1</sup> Charlotte Karlsson,<sup>1</sup> Hanna Betts Lindroos,<sup>1</sup> Sara Wedahl,<sup>1</sup> Yuki Katou,<sup>2</sup> Katsuhiko Shirahige,<sup>2</sup> Camilla Sjögren<sup>1\*</sup>

Sister-chromatid cohesion, established during replication by the protein complex cohesin, is essential for both chromosome segregation and double-strand break (DSB) repair. Normally, cohesion formation is strictly limited to the S phase of the cell cycle, but DSBs can trigger cohesion also after DNA replication has been completed. The function of this damage-induced cohesion remains unknown. In this investigation, we show that damage-induced cohesion is essential for repair in postreplicative cells in yeast. Furthermore, it is established genome-wide after induction of a single DSB, and it is controlled by the DNA damage response and cohesin-regulating factors. We thus define a cohesion establishment pathway that is independent of DNA duplication and acts together with cohesion formed during replication in sister chromatid-based DSB repair.

The tethering of sister chromatids by the cohesin complex, so called sister-chromatid cohesion, is essential for chromosome segregation (1). Cohesin consists of Smc1, Smc3, Mcd1 (also called Scc1), and Scc3 and is loaded onto chromosomes before replication by Scc2 and Scc4 (2). The establishment of cohesion requires Eco1 (also called Ctf7) and occurs in the S phase of the unchallenged cell cycle (3–8). Cohesion then persists until anaphase, when it is resolved by proteolytic cleavage of Mcd1, which is triggered by the degradation of Pds1 (9–11). In addition to its central role in chromosome segregation, replication-established cohesion is needed for double-strand break (DSB) repair in postreplicative cells (12). Cohesin also has to be recruited to the site of damage for efficient repair (13, 14), and de novo cohesion is established in G<sub>2</sub>/M cells exposed to ionizing irradiation (13). This raises the possibil-

ity that chromatid-based DSB repair requires both cohesion formed during replication and postreplicative damage-induced cohesion. It also challenges present concepts that cohesion establishment is tightly connected to chromosome duplication. Therefore, we investigated how damage-induced cohesion is regulated and resolved its function in DSB repair and chromosome segregation.

Central to our investigations are experimental systems in which damage-induced cohesion can be distinguished from cohesion formed during replication (fig. S1, A to C). In one of these systems, *smc1-259* temperature-sensitive cells are first arrested in G<sub>2</sub>/M at permissive temperature. Thereafter, temperature-resistant, damage-induced cohesion is generated by the expression of wild-type (WT) *SMC1* and treatment with  $\gamma$ -irradiation (Fig. 1, A and B, and fig. S1A) (13). We first ascertained that our results were not influenced by the absence of a mitotic spindle in nocodazole-arrested cells (Fig. 1, A and B). Thereafter, we investigated the function of central DNA damage-response proteins in damage-induced cohesion. Mre11 is one of the first proteins that localizes at a DSB (15) and is essential for the recruitment of cohesin to the damage

(14, 16). Accordingly, damage-induced cohesion was compromised in *mre11 $\Delta$*  cells (Fig. 1C) (17). Other regulators of the DNA damage response that influence cohesin's break localization are the Tel1 and Mec1 kinases, which phosphorylate histone 2A (H2A) (in humans, H2AX) (14, 18). Phosphorylated H2A ( $\gamma$ -H2A) marks the DSB and is required for DSB recruitment of cohesin (14). Correspondingly, the formation of damage-induced cohesion was defective in cells lacking Tel1 or Mec1 or in cells expressing nonphosphorylatable H2A (Fig. 1, D to F). However, in the absence of Tel1 or Mec1, substantial amounts of  $\gamma$ -H2A and cohesin still accumulate at a DSB because of the overlapping function of the other kinase (14, 18). This indicates that Tel1 and/or Mec1 could influence cohesion in a way other than through  $\gamma$ -H2A-dependent recruitment of cohesin. The two kinases also activate Rad9, which in turn transmits the signal to downstream events in the DNA damage response (19–21). Damage-induced cohesion was, however, unaffected in *rad9 $\Delta$*  cells (Fig. 1G), showing that if Mec1 and/or Tel1 affect damage-induced cohesion independently of cohesin recruitment, this pathway does not include the activation of Rad9.

To determine whether replication induced by the repair process influences cohesion, we investigated damage-induced cohesion in *rad52 $\Delta$*  cells. Rad52 facilitates the direct interaction between the DNA flanking a DSB and an undamaged homologous template, which is essential for eliciting DNA synthesis at the break (22, 23). Therefore, the unperturbed formation of cohesion in *rad52 $\Delta$*  cells (Fig. 1F) shows that, in contrast to the establishment process in unchallenged cells, damage-induced cohesion is independent of ongoing DNA duplication (17).

We observed chromatid separation in a limited region of chromosome V (chr. V) that experiences roughly one DSB per cell at the irradiation dose applied (13). Because cohesin is recruited to only 50 to 100 kb around the DSB (13, 14), the  $\gamma$ -ray-induced cohesion suggests a more general activation of cohesin (Fig. 1, A and B). To investigate whether a single genomic DSB triggers cohesion, we used an uncleavable

<sup>1</sup>Department of Cell and Molecular Biology, Karolinska Institute, 171 77 Stockholm, Sweden. <sup>2</sup>Gene Research Centre, Tokyo Institute of Technology, 4259 Nagatsuta, Midori-ku, 226-8501 Yokohama, Japan.

\*To whom correspondence should be addressed. E-mail: camilla.sjogren@ki.se